Salt Leaching As a Green Method for The Production of Polyethylene Foams for Thermal Energy Storage Applications

Alessandro Sorze
University of Trento Department of Industrial Engineering: Universita degli Studi di Trento Dipartimento di Ingegneria Industriale
Francesco Valentini (francesco.valentini@unitn.it)
Universita degli Studi di Trento https://orcid.org/0000-0001-9496-0501
Andrea Dorigato
University of Trento Department of Industrial Engineering: Universita degli Studi di Trento Dipartimento di Ingegneria Industriale
Alessandro Pegoretti
University of Trento Department of Industrial Engineering: Universita degli Studi di Trento Dipartimento di Ingegneria Industriale

Research Article

Keywords: foams, polyethylene, phase change materials, thermal energy storage, salt leaching

Posted Date: July 14th, 2021

DOI: https://doi.org/10.21203/rs.3.rs-680156/v1

Version of Record: A version of this preprint was published at Polymer Engineering & Science on March 10th, 2022. See the published version at https://doi.org/10.1002/pen.25953.

Journal of Polymers and the Environment, to be submitted

Salt leaching as a green method for the production of polyethylene foams for thermal energy storage applications

Alessandro Sorze, Francesco Valentini*, Andrea Dorigato, Alessandro Pegoretti*

University of Trento, Department of Industrial Engineering and INSTM Research Unit
Via Sommarive9 38123 Trento (Italy)

* Corresponding authors:
F. Valentini (e-mail: francesco.valentini@unitn.it)
A. Pegoretti (e-mail: alessandro.pegoretti@unitn.it)

Abstract

Materials able to store thermal energy can be a useful strategy in order to reduce energy consumption of buildings and to decrease greenhouse gases emissions. In this work, for the first time, the technique of salt leaching has been used for the production of novel polyethylene foams containing different amounts of a microencapsulated phase change material (PCM) with a melting point of 24 °C, to be potentially applied in building insulation. The microstructural, thermal and mechanical properties of the produced foams have been comprehensively investigated. The prepared foams were characterized by high values of open porosity (about 60 %) and by density values around 0.4 g/cm^3. Differential scanning calorimetry tests revealed that the adopted production process caused a partial loss of PCM, resulting in an effective PCM content of around 33 % for the sample with the highest PCM loading (56 wt%). Infrared thermography analysis demonstrated that the time required from the samples to reach a set temperature, thanks to the presence of PCM, was up to two times higher with respect to the reference foam. Shore-A measurements evidenced that the addition of PCM generally led to a softening of the foams. Tensile mechanical tests confirmed the softening effect provided by the addition of the microcapsules, with a decrease of the stiffness and of the strength of the material. Interestingly, strain at break values were considerably increased upon PCM introduction.

Keywords: foams, polyethylene, phase change materials, thermal energy storage, salt leaching.

1 Introduction

Recently, the improved living conditions of people and the increase of growth rate of population have led to an enhancement of the energy demands for buildings. Recent studies have found that the primary source of energy in the world will continue to be fossil fuels up to 2030 [1]. The development of sustainable building and renewable energy resources is thus becoming an important issue for our society. In fact, the building sector is one of the most energy consuming, with an overall energy consumption of 30 % in the world[1] (40 % in Europe [2]) and it is responsible for one-third of the worldwide emissions of greenhouse gases[3]. Considering that the annual solar energy incident on buildings is greater than the energy needs for hot water and heating, the possibility of a thermal management of renewable energy is a crucial point both in building and automotive sectors in order to minimize energy consumption and toxic gases emissions [4, 5]. The ability of a material to temporarily store heat and release it in a second time is a process called thermal energy storage (TES) [4, 6, 7]. In order to store large amounts of thermal energy, latent heat thermal energy storage systems are particularly promising, because of their capacity to store heat at constant temperature upon a phase change in the material. Phase change materials (PCMs) are thus designed for the storage of a considerable amount of heat when they undergo a reversible solid-to-liquid transition at a constant temperature [8-12]. Examples of PCMs are paraffin waxes [13-16], fatty acids [17], polyethylene glycol (PEG) [18], fatty alcohols [19], salt hydrates and metals [12, 20]. Paraffins are organic PCMs and they are widely used for thermoregulation of buildings [10, 21], sportswear [22] and smart fabrics [23-25], thanks to their low cost, high heat of fusion, cheapness, non-corrosive behaviour, chemically inertness, thermal stability, little volume changes on melting and low vapor pressure in the molten state [8, 9, 26, 27]. PCMs can be encapsulated in order to avoid leakage above the melting temperature, increasing thus their strength, their durability and thermal stability, their easy-handling and reliability [25, 28, 29]. A second strategy to avoid PCM leakage is the shape stabilization [15, 30, 31]: it consists in the confinement of the PCM within a polymer matrix, such as high-density polyethylene [32], polypropylene [33], poly(methylmethacrylate) [34], polyurethane copolymers [35], acrylic resins[36], styrene–butadiene–styrene rubber and ethylene-propylene-diene-monomer (EPDM) rubber [13].

Polymeric foams are expanded materials in which the porosity is obtained using chemical or physical blowing agents. In comparison with bulk polymers they present low density, low thermal conductivity, high insulation capacity, elevated thermal stability and also good mechanical properties in terms of toughness and impact resistance [37]. In recent years, polyolefins have found wide interest as matrices for the foaming process. In fact, polyolefin foams are characterized by a

wide range of properties that allow them to be employed as insulation materials in various fields such as buildings, automotive, military, aerospace, aircraft, sports etc. [38, 39]. Polyethylene foams are generally used for production of gaskets and vibration pads, sound insulation, water barriers, expansion joints, pipe insulation, glazing seals. They are used in a wide range of density from 0.15 to 0.60 g/cm^3 [40]. Physical blowing agents are inert gases, which are introduced into the polymer matrix during a saturation process, usually at high pressure [37]. The most widely used physical blowing agents are nitrogen (N_2), carbon dioxide (CO_2) or hydrocarbons such as pentane. Chemical blowing agents are powders that can induce an exothermic or endothermic reaction inside the polymer matrix through their thermal decomposition, generating thus a gas phase. The most common one is azodicarbonamide (ADC) which decomposes at around 170-200 °C and possesses high gas yield, releasing nitrogen and heat [38, 41-43]. Examples of endothermic chemical blowing agents are sodium bicarbonate and zinc bicarbonate [44]. Despite the extensive use of chemical foaming agents for the production of expanded polymers, many of them are hazardous for health and their use is not allowed in the EU [43]. For this reason, safer physical foaming agents, like water or hydrocarbons, are often required [45, 46]. However, physical blowing agents generally show some problems related to the difficult manufacturing process and the use of additional and expensive equipment [43].

A possible environmentally friendly alternative to traditional foaming agents is represented by the "salt leaching" technology, which involves the addition of water-soluble salt particles (such as sodium chloride, potassium chloride, etc) into the polymer matrix and their subsequent dissolution in hot water, leading to the formation of a porous cellular structure within the polymer matrix [47-50].This technology has been widely used for the production of scaffolds [48, 49, 51], plastic semiconductors [52], open cell nitrile-butadiene-rubber (NBR) sponges [53], EPDM foams [54, 55], applied in tissue engineering and for soft sensors [56]. By tuning the polymer-to-salt ratio and by varying the leachable particle size, the porosity of the resulting scaffolds may range between 70 % and 95 %. Moreover, salt leaching maybe used in combination with other techniques (gas foaming, compression moulding) in order to further modify the structure of the foams, increasing the pore interconnectivity [57].

Despite the environmental advantages that could arise from the combination of polyethylene foams produced through particle leaching and the thermal energy storage capability through the addition of PCM within the polymeric matrix, no studies can be found in the open literature on this topic. This work is thus focused on the development of polyethylene foams produced through salt leaching technique and containing different amounts of a microencapsulated PCM with a melting

point of 24 °C. The resulting materials could be potentially applied for the thermal management in the building sector and as thermo-acoustic insulators for thermal plants. The microstructural behaviour of the prepared foams was correlated to their thermal and mechanical properties.

2 Experimental part

2.1 Materials

High density polyethylene (HDPE) ELTEX A4040P (density = 0.94 g/cm^3, melt flow index (MFI) at 190ºC/2.16 kg = 3.5 g/10min) was purchased from Ineos polyolefins (Rolle, Switzerland) in form of fine powder. Polyethylene glycol (PEG) in form of granules, having a molecular weight of 2000 Da, was acquired from Alfa Aesar (Kandel, Germany) and used to improve the leaching efficiency. Sodium chloride, commercial grade (density = 2.16 g/cm^3), was grinded and sieved using a 230-mesh sieve in a granulometry lower than 63 µm. Preliminary tests were carried out in order to determine the granulometry value that allowed to minimize the density of the foam and a salt size lower than 63 µm was thus selected. The salt particles were then dried and stored in an oven at 60 °C until use. MPCM24 microcapsules containing a wax with a melting point of 24 °C and a melting enthalpy of 145 J/g were purchased from Microtek Laboratories Inc. (Dayton, OH, USA) and used as phase change material. Polyethylene powder, PEG and microcapsules were used as received.

2.2 Samples preparation

Polyethylene foams were prepared by melt compounding in an internal mixer (Thermo HaakeRheomix® 600), equipped with counter rotating rotors. The compounding process was performed at a temperature of 153 °C and a rotor speed of 50 rpm. The polymer matrix and the PCM were manually mixed and then added to the melt compounder, where they were mixed for 5 minutes. Salt and PEG were then gradually added into the mixer, reaching a total mixing duration of 20 minutes. The total amount of materials inserted in the mixing chamber was of about 40 g. The resulting compounds were then compression moulded at a temperature of 180 °C for 13 minutes. The pressure was set at 1 bar for the first 3 minutes and at 7 bar and for the next 10 minutes. In this way, square sheets of polyethylene (dimensions of 100x100x2 mm^3) with different PCM amounts were obtained. The leaching method described by Scaffaro et al. [49] was taken as a reference for the present work. Pressed samples were thus immersed in boiling demineralized water for 3 hours in order to obtain a proper salt dissolution. The obtained foams where then dried overnight in an oven at 60 °C.

The list of the samples with their codes is reported in Table 1. Their designation is formed by the term PE followed by the average size of the salt particles (< 63 μm) used for the foams production and by the PCM content expressed in phr (per hundred resin).

2.3 Experimental methodologies

2.3.1 Residual salt and water uptake measurements

The amount of residual salt (*RS*) not dissolved during the leaching process has been calculated according to the Equation (1):

$$RS = \frac{m_{dry} - m_{tot}}{m_{dry}} \quad (1)$$

where m_{dry} is the mass of the material after the drying process subsequent to the leaching and m_{tot} is the theoretical mass of the material in the case of complete salt dissolution, evaluated according to Equation (2):

$$m_{tot} = m_0 - m_{NaCl} - m_{PEG} \quad (2)$$

where m_0 is the mass of the sample before salt leaching, m_{NaCl} is the initial mass of the salt in the blend (30 g) and m_{PEG} is the initial mass of the PEG in the blend (2 g). With the aim of evaluating the continuity of the porosity and therefore the dissolution of the foaming agents (PEG, NaCl), also a foam connectivity parameter (*C*) has been calculated according to Equation (3)[49]:

$$C = \frac{(m_0 - m_{dry})}{m_{NaCl} + m_{PEG}} \quad (3)$$

Water uptake measurements were carried out in order to identify the influence of the porosity on the water absorption tendency of the foams. These tests were carried out following the procedure reported in the ASTM D570 standard: samples were previously dried for 24 hours in oven at 50 °C and then weighted, they were then immersed in demineralized water for a certain amount of time, and then weighted again. The mass of the samples was measured using a Kern KB3600 balance (resolution of 10 mg). For each sample the mass measurements were carried out after immersion in water for 30 minutes, 1 hour, 2 hours, 8 hours and 24 hours. The water uptake (*WU*) has been calculated according to Equation (4):

$$WU = \frac{m_{wet} - m_{dry}}{m_{dry}} \quad (4)$$

where m_{wet} is the mass of the sample after the immersion in water and m_{dry} is the mass of the sample after drying.

2.3.2 Morphological properties

Cryofractured surfaces of the foams were observed through a Zeiss Supra 40 field emission scanning electron microscope (FESEM), operating at an accelerating voltage of 2.5 kV inside a chamber under a vacuum of 10^{-6} Torr. Before the observations, the samples were metallized through the deposition of a thin electrically conductive Pt/Pd coating.

Helium pycnometry density (ρ_{picn}) measurements were conducted using a gas displacement AccuPycII 1330 pycnometer (Micrometrics Instrument Corporation, USA) at a temperature of 23 °C. For each sample 30 replicate measures were performed. Geometrical density (ρ_{geom}) (i.e. mass over the total volume inclusive of solid, closed and open porosity) was carried out on five cylindrical specimens (18 mm in diameter), by measuring their mass with a Gibertini E42 balance (0.1 mg sensitivity) and their dimensions using a digital calliper with a resolution of 0.01 mm.

Residual salt was taken into account for the density measurements; therefore, mixture rule (Equation 5) has been used.

$$\rho_F = \frac{W_F}{\frac{1}{\rho_c} - \frac{W_{RS}}{\rho_{RS}}} \tag{5}$$

where ρ_F is the effective density of the foam considering the residual salt content, ρ_c is the geometric density of the foam (containing residual salt), W_{RS} and W_F are the weight fraction of residual salt and expanded material (without residual salt), respectively, and ρ_{RS} is the density of salt (2.16 g/cm^3)[58]. According to ASTM D6226 standard, it was possible to calculate the total porosity (P_{tot}) and the fraction of open porosity (OP) and closed porosity (CP) according to Equations (6-8):

$$P_{tot} = 1 - \frac{\rho_{geom}}{\rho_{bulk}} \tag{6}$$

$$OP = 1 - \frac{\rho_{geom}}{\rho_{picn}} \tag{7}$$

$$CP = P_{tot} - OP \tag{8}$$

where ρ_{bulk} is the density of the non-expanded polymer matrix (equal to 0.914 g/cm^3) obtained from pycnometric measurements.

2.3.3 Thermal properties

Investigation of the thermal degradation behaviour of the prepared materials was carried out through thermogravimetric analysis (TGA) using a Mettler TG50 thermobalance under a nitrogen flow of 10 ml/min in a temperature range between 30 and 700 °C, at a heating rate of 10 °C/min.

The temperature associated to a mass loss of 5% ($T_{5\%}$), the temperatures associated to the maximum rate of degradation of the PCM and of the PE matrix (respectively denoted as T_{peak1}, T_{peak2}) and the residual mass at 400 °C (m_{400}) were determined.

Differential scanning calorimetry (DSC) measurements were performed on the prepared samples using a Mettler DSC30 calorimeter under a nitrogen flow of 100 ml/min. A first heating scan from -30 to 70 °C was followed by a cooling stage from 70 to -30 °C and by a second heating scan from -30 to 70 °C. All the thermal ramps were carried out at 10 °C/min. In this way, the melting temperature of the PCM during the first and the second heating scan (T_{m1},T_{m2}), its crystallization temperature ($T_{c,}$) and its specific melting and crystallization enthalpy values ($\Delta H_{m1,}$ $\Delta H_{c,}$ ΔH_{m2}) were obtained. Moreover, the effective PCM content in the foams was determined during the first heating scan (PCM_{m1}^{eff}), the cooling scan (PCM_{c}^{eff}) and the second heating scan (PCM_{m2}^{eff}) as the ratio between the specific enthalpy of the samples and the corresponding specific enthalpy values of the neat PCM, as shown in Equations (9-11):

$$PCM_{m1}^{eff} = \frac{\Delta H_{m1}}{\Delta H_{m1PCM}} \quad (9)$$

$$PCM_{c}^{eff} = \frac{\Delta H_{c}}{\Delta H_{cPCM}} \quad (10)$$

$$PCM_{m2}^{eff} = \frac{\Delta H_{m2}}{\Delta H_{m2PCM}} \quad (11)$$

where ΔH_{m1PCM}, ΔH_{cPCM}, ΔH_{m2PCM} are the specific phase change enthalpy values of the neat PCM collected during the first heating scan, the cooling and the second heating scan, respectively.

The thermal energy storage performance of the materials was investigated monitoring their surface temperature evolution using an infrared thermal camera FLIR E60 (emissivity = 0.86). The specimens were heated in an oven at 40 °C overnight and then inserted in a climatic chamber at a temperature of 5 °C; their surface temperature was then monitored until the thermal equilibrium between the samples and the environment was reached. In the same way, the specimens were cooled in a refrigerator at 0 °C overnight and then inserted in an oven at a temperature of 40 °C. In the heating tests the time required to reach a temperature of 40 °C (t_{40}) has been evaluated, in the cooling tests the time required to reach a temperature of 5 °C (t_5) has been determined.

2.3.4 Mechanical properties

Shore A hardness test was performed using a Hilderbrand Prufstander OS2 durometer following the ASTM D2240 standard. Square samples 20 mm wide and 2 mm thick were tested, and Shore A hardness value was determined after a loading time of 5 seconds. At least five measurements were performed for each composition.

Tensile properties of the prepared foams under quasi-static conditions were measured on ISO 527 type 1BA dumbbell specimens (gage length equal to 30 mm) using an Instron 5969 tensile testing machine equipped with a load cell of 100 N and operating at a cross-head speed of 1 mm/min. The elastic modulus (E) has been calculated as a secant modulus between strain values of 0.0005 mm/mm and 0.0025 mm/mm. The stress at break (σ_R) and the strain at break (ε_R) have been also evaluated. At least five specimens were tested for each composition. Both the elastic modulus and the stress at break values were normalized for the geometrical density of the foams.

3 Results and discussion

3.1 Residual salt and water uptake measurements

Table 2 shows the residual salt and the connectivity values obtained for the prepared foams, evaluated according to Equations (1-3). It is possible to observe that the percentage of residual salt does not depend on the PCM content and it is around 10-13 % for all the samples, except for PE_<63s_100_p foam that is characterized by a higher residual salt content (around 27 wt%), probably because of an inhomogeneous salt dispersion during the production stage. However, the connectivity decreases as the content of PCM inside the foam increases, passing from 80% for the neat PE foam up to 47% for the PE_<63s_130_p sample. This could be explained by the fact that the PCM filled some of the pores, thus limiting the interconnections among them.

In Figure 1 the water uptake values, calculated according to Equation (4), are reported as function of the testing time. In this plot, also the water uptake of the bulk polyethylene sample (PE) is reported. The parabolic shape of the curves indicates that the water absorption in these foams is mainly governed by a diffusion mechanism [59] and that the absorption rate decreases with time, reaching in some cases a plateau after 24h. As it could be expected, the bulk PE sample does not absorb water, in fact the water uptake value after 24 hours is zero. It is interesting to notice that increasing the PCM amount inside the foams, the water uptake decreases. This could suggest that the addition of more PCM leads to a decrease in the porosity and thus, in the volume available for

water absorption. This feature can be also correlated to the decrease of the connectivity observed in Table 2. In fact, the increase of the PCM content in the foams leads to the formation of a less interconnected structure and thus to a lower water absorption capability.

3.2 Morphological properties

The morphological features of the foamed samples were studied through scanning electron microscopy (SEM) observations. In Figure 2(a-f) representative SEM micrographs at 500x and 5000x of the foamed samples are reported. It is possible to observe that the prepared foams are characterized by an open porosity with pores dimension, in the case of the PE sample, of 21.4 ± 14.7 µm, that decreases upon PCM addition reaching a value of 10.1 ± 4.1 µm for the PE_<63s_130_p foam. Moreover, from Figure 2d a poor adhesion between paraffin microcapsules and the PE matrix, together with an evident interfacial debonding, can be observed. It has to be considered that the PCM is contained in a melamine-formaldehyde shell, probably characterized by a limited chemical compatibility with polyolefin matrices. In general, few capsules can be detected in these micrographs, meaning that PCM distribution is not homogeneous in the foams but also that part of PCM could have been lost during the melt compounding and the subsequent leaching process. However, the morphology of the prepared foams is quite similar to that of PLA scaffolds produced by Scaffaro et al. through the salt leaching method using a salt grain size of 45-65 µm [49]. In both cases, indeed, materials are characterized by an elevated degree of interconnected pores, with very thin cell walls. The addition of PCM in the foams leads to a less porous structure, since paraffin capsules are bulk materials that occupy some of the pores (see Figure 2e). Moreover, the addition of PCM results in an increase of the residual salt concentration, clearly visible in Figure 2f in form of cubic particles. These residues did not dissolve during salt leaching, because they are too small (about 4.5 µm) and also because PCM particles could have hindered in some way the complete leaching of salt granules.

From the results of density measurements, shown in Figure 3a it is possible to notice, the geometrical density increases with the PCM amount, since the microencapsulated paraffin remains in the foam after salt leaching technique filling some of the pores. On the other hand, the pycnometric density values are practically unaffected by the content of PCM in the foams and are systematically higher than the corresponding geometric density values. This could be explained by the fact that, with the salt leaching method, the produced foams have an elevated degree of

interconnection of the pores (see Table 2) and an open pores structure (see Figure 2). In these conditions, the density values obtained through pycnometric measurements are close to bulk density of PE (taking also into account the PCM content and the residual salt concentration).

Figure 3b shows the total and open porosity values of the foams as a function of PCM content, evaluated according to Equations (6) and (7). It is possible to notice that increasing the PCM content, the porosity values decrease, since PCM microcapsules occupy some of the pores. For example, comparing PE_<63s and PE_<63s_130_p foams, the total porosity passes from 65 % to 45 % upon the PCM addition. On the other hand, the total and the open porosity values for every sample are quite similar, meaning that the closed porosity is practically negligible in all the produced samples. This effect was also observed in a previous work where the salt leaching technique was used for the production of EPDM rubber foams [54].

3.3 Thermal properties

Thermogravimetric curves of the prepared foams, along with the corresponding derivative plots are presented in Figure 4(a,b) while the most significative results are listed in Table 3 and Table 4. Comparing PE and PE<63s samples, it is evident that the foaming stage produces a slight decrease of the thermal stability of the sample, with a shift of thermogravimetric curves towards lower temperatures. This behaviour can be explained considering the increased surface area exposed to degradation in the case of foams, the presence of preferential pathways for release of by-products due to the presence of an open porosity and the oxidative processes due to the air entrapped in the pores[54, 60]. From Figure 4a a first degradation stage, between 200°C and 400°C, can be seen only in the foamed samples with PCM, and this is associated with PCM degradation (T_{peak1}), while a second degradation stage, corresponding to the degradation of the PE matrix occurs at about 485 °C (T_{peak2}). From the results reported in Table 3 it is evident that both T_{peak1} and T_{peak2} are not substantially affected by the PCM content in the foams. As it could be expected, the thermal degradation stability of the foams is negatively influenced by the PCM addition. As it can be seen in Table 3, the values of $T_{5\%}$ decrease as the content of PCM increases (from 398 °C in the case of PE<63s sample to 185 °C for the PE_<63s_130_pfoam). It should be considered that these temperature values are much higher than those reached in an eventual application in buildings of these foams, and the observed drop of the thermal stability should not dramatically limit their technical employability of the prepared foams in this field.

It is also possible to check if the mass loss values between 200 and 400 °C are coherent with the PCM content in the foams. From the m_{400} values detected for PE_<63s_25_p,PE_<63s_50_p and PE_<63s_100_p foams, it is possible to conclude that the PCM content within the foams is, respectively, 10.4 %, 22.7 %, 40.6%. These values are comparable with the PCM contents reported in Table 1 and re-calculated considering the residual salt content in each sample (i.e., 16.0 %, 28.9 %, 37.4 %, respectively). In the case of PE_<63s_100_p foam, the mass loss value is slightly higher than the nominal PCM content and this result can be explained by an inhomogeneous distribution of PCM inside the sample. For the PE_<63s_130_p foam, the PCM content is 35.3 %, much lower than the expected one (i.e., 49.0 %, value of Table 1 re-calculated considering the residual salt content in the sample), meaning that some PCM could have been lost during the compounding operations and the subsequent leaching process.

DSC curves of the prepared samples and of the neat PCM are presented in Figure 5(a-c) and the most significant results are summarized in Table 4. In Figure 5a and 5c the first and second heating scans are reported and in both figures two endothermic peaks can be observed. The first peak, approximately at 20-25 °C, is associated to the melting of paraffin and its intensity increases with the PCM content in the foams. The second peak, observed at around 50 °C, is associated to the melting of PEG that remained in the foam and has not been fully dissolved.

In Figure 5b the thermograms referred to the cooling scan are represented. In this case a double exothermic peak in the temperature interval from -15 °C to 20 °C, corresponding to the crystallization of the PCM, can be noticed, and its intensity increases with the PCM amount. As it could be expected, the melting/crystallization enthalpy values increase with the PCM amount, and the PE_<63s_130_p foam shows a ΔH_{m1} value of 50 J/g. However, taking into account the PCM weight concentration within the foams, reported in Table 1, it is possible to see that ΔH_{m1}, ΔH_c, ΔH_{m2} values are systematically lower than the expected ones. Consequently, the effective PCM contents (PCM_{m1}^{eff}, PCM_{c}^{eff}, PCM_{m2}^{eff}) are considerably lower than to the nominal values reported in Table 1. For instance, the sample PE_<63s_130_p has a PCM_{m1}^{eff} value of 33 % (instead of 56 %) and the sample PE_<63s_25_p a value of 1.6 % (instead of 20 %). These discrepancies are partly due to the presence of residual salt that reduces the effective PCM content and also due to the PCM loss during the production process of samples. Considering that TGA tests highlighted that the differences between the real and the theoretical PCM contents within the samples are realtively

small, the discrepancy detected in DSC tests can be also attributed to the breakage of some capsules during the preparation stage. In other words, the paraffin that flew out of the capsules is not able to melt/crystallize within the PE matrix in an efficient way.

The melting temperature of PCM (T_{m1} and T_{m2}) slightly increases with the PCM amount. On the other hand, the crystallization temperature (T_c) decreases as the PCM content increases. This trend is not due to an intrinsic property of the material, but rather than to the lower thermal conductivity of the foams with respect to the neat PCM. In these conditions, all the thermal transition are shifted towards higher temperature in the heating scan and to lower temperature in the cooling stage. A similar behaviour was also observed for PCM microcapsules dispersed in an acrylic matrix reinforced with carbon-fibres, that showed lower crystallization temperature with respect to neat PCM microcapsules[61]. The melting enthalpy values in the first and second heating ramps (ΔH_{m1} and ΔH_{m2}) are quite similar, meaning that the capability of samples to store heat is retained even when the thermal history of the samples is deleted. Further tests will be made in the future to evaluate the retention of the TES properties upon the application of repeated thermal cycles.

Figure 6 (a-f) reports the result of the thermal imaging tests for the PE_<63s_130_p sample. In particular, Figures 6(a-c) show pictures taken after 0, 3 and 10 minutes during the heating scan, while Figures 6(d-f) represent pictures taken after 0, 3 and 10 minutes during the cooling test. This analysis allows to investigate the evolution of the surface temperature of the foams upon heating/cooling stages, in order to better evaluate their effective capability to store/release heat. Moreover, through this analysis it is possible to evaluate the PCM distribution inside the foam, that corresponds to the colder spots during the heating scan and to the hotter spots during the cooling stage. Looking at Figures 6(a,b) and (d,e), the inhomogeneous distribution of PCM within the foams can be clearly identified. The reason for this inhomogeneity can be the elevated salt content that was added during the mixing process, that hinders the homogeneous distribution of the PCM within the PE matrix.

Figure 7(a,b) report the temperature profiles obtained during the thermal imaging tests on the prepared foams, while the most significant results are listed in Table 5. Increasing the amount of PCM inside the foam, both heating and cooling curves are delayed along the time scale. Moreover, in samples containing PCM, an isothermal step corresponding to the phase transition of paraffin at a temperature of around 24°C can be clearly observed. The results reported in Table 5 highlight that PE_<63s_130_p foam is characterized by values of t_5 and t_{40} which are double in comparison to

those of the foam without PCM. The results indicate that, even if part of the PCM was lost during the production process (or it is not able to melt/crystallize once inserted in the PE matrix), the prepared foams are able to store/release an interesting amount of thermal energy in the considered temperature interval.

3.4 Mechanical properties

From the stress-strain curves presented in Figure 8 and from the results reported in Table 6, it is possible to observe that foamed samples without PCM possess the highest specific elastic modulus (183 MPa·cm^3/g) and specific strength (4.8 MPa·cm^3/g). The addition of PCM inside the foam leads to a progressive decrease of the specific strength and of the specific elastic modulus. In particular, the specific elastic modulus decreases from 182.7 MPa·cm^3/g down to 57.4 MPa·cm^3/g in the case of PE_<63s_130_p sample. This behaviour could be explained by the lower stiffness and strength of the microcapsules compared to the neat PE matrix [62]. The same conclusion can be drawn if Shore A values, reported in Table 6, are considered. Shore A value for the PE_<63s is 80, while it drops down to 67 if the PE<63s_130p foam is considered.

In a similar way, the specific strength decreases from 4.8 MPa·cm^3/g up to 1.9 MPa·cm^3/g for the PE<63s_130p sample. The decreased strength of the foams due to PCM addition can be probably explained by the limited interfacial adhesion between the PE matrix and the PCM microcapsules, as detected in SEM micrographs (see Figure 2f). Interestingly, the strain at break values of the foams are considerably increased with the PCM addition, passing from 0.08 mm/mm in the case of PE_<63s sample up to 0.16 mm/mm for the PE_<63s_130_p foam. It can be hypothesized that the observed increase in the strain at break values upon PCM addition can be attributed to the toughening mechanism produced by the interfacial debonding between the PE matrix and the microcapsules at elevated deformation levels. In these conditions, a considerable amount of energy must be spent to create debonding surfaces wihin the samples, with a consequent fracture resistance increase. However, further tests will be required to have a better comprehension of this effect. It is therefore possible to conclude that the addition of paraffin microcapsules within these materials plays a softening effect, with a consistent reduction of the dimensional stability and of the failure resistance, accompanied by an interesting improvement of the ultimate strain levels.

5 Conclusions

This work demonstrated that the salt leaching technique could be a very interesting method for the sustainable production of polyethylene foams applied in thermal energy storage applications. Evaluation of water uptake, SEM micrographs and density measurements allowed to investigate the morphology of the foamed samples, showing that the produced foams were characterized by an open porosity with an interconnected structure. The presence of PCM in the foams filled part of the pores, increasing thus the foam density and reducing water absorption values. Thermogravimetric analysis evidenced that the thermal degradation stability decreased with the PCM amount, but the degradation temperature remained well above the maximum working temperature of these foams in building applications. DSC analysis showed that these materials were able to store/release an interesting amount of thermal energy, even if the measured melting/crystallization enthalpy value were below the theoretical ones. Infrared thermography analysis highlighted that the time required by the PE_<63s_130_p sample to reach the set temperatures was doubled with respect to the neat PE foam. The stiffness, the hardness and the strength of the foams were considerably reduced upon the PCM addition, probably due to the limited intrinsic mechanical properties of the microcapsules and the low of interfacial adhesion between the PCM and the PE matrix. Interestingly, the strain at break values were noticeably improved upon PCM addition. It could be therefore concluded that the prepared foams possessed interesting thermo-mechanical features, and they could be successfully applied for the thermal insulation and the thermal management of buildings. An optimization of the production process should be made in the future to increase the PCM concentration within the foams and to improve the interfacial adhesion between the capsules and the PE matrix.

Acknowledgements

Ms. Claudia Gavazza is gratefully acknowledged for the acquisition of SEM micrographs.

Declarations

Fundings

The author(s) received no financial support for the research, authorship, and/or publication of this article.

Conflict of interest

The authors declare that they have no conflict of interest.

Availability of data and material

The authors declare that the manuscript has no associated data.

Ethics approval

The authors declare that the manuscript does not contain any studies with human participants or animals performed by any of the authors.

References

1. Memon, S.A., *Phase change materials integrated in building walls: A state of the art review.* Renewable and Sustainable Energy Reviews, 2014. **31**: p. 870-906.
2. Soares, N., et al., *Review of passive PCM latent heat thermal energy storage systems towards buildings' energy efficiency.* Energy and Buildings, 2013. **59**: p. 82-103.
3. Alexiadis, A., *Global warming and human activity: A model for studying the potential instability of the carbon dioxide/temperature feedback mechanism.* Ecological Modelling, 2007. **203**(3-4): p. 243-256.
4. Hongois, S., et al., *Development and characterisation of a new MgSO4−zeolite composite for long-term thermal energy storage.* Solar Energy Materials and Solar Cells, 2011. **95**(7): p. 1831-1837.
5. Jankowski, N.R. and F.P. McCluskey, *A review of phase change materials for vehicle component thermal buffering.* Applied Energy, 2014. **113**: p. 1525-1561.
6. Anisur, M.R., et al., *Curbing global warming with phase change materials for energy storage.* Renewable and Sustainable Energy Reviews, 2013. **18**: p. 23-30.
7. Fernandes, D., et al., *Thermal energy storage: "How previous findings determine current research priorities".* Energy, 2012. **39**(1): p. 246-257.
8. Peng, S., A. Fuchs, and R.A. Wirtz, *Polymeric phase change composites for thermal energy storage.* Journal of Applied Polymer Science, 2004. **93**: p. 1240-1251.
9. Bo, H., E.M. Gustafsson, and F. Setterwall, *Phase transition temperature ranges and storage density of paraffin wax phase change materials.* Energy, 1999. **24**(12): p. 1015-1028.
10. Borreguero, A.M., et al., *Improvement of the thermal behaviour of gypsum blocks by the incorporation of microcapsules containing PCMS obtained by suspension polymerization with an optimal core/coating mass ratio.* Applied Thermal Engineering, 2010. **30**(10): p. 1164-1169.
11. Dorigato, A., et al., *Polyethylene wax/EPDM blends as shape-stabilized phase change materials for thermal energy storage.* Rubber Chemistry and Technology, 2017. **90**(3): p. 575-584.
12. Milián, Y.E., et al., *A review on encapsulation techniques for inorganic phase change materials and the influence on their thermophysical properties.* Renewable and Sustainable Energy Reviews, 2017. **73**: p. 983-999.

13. Valentini, F., A. Dorigato, and A. Pegoretti, *Novel EPDM/paraffin foams for thermal energy storage applications.* Rubber chemistry and technology, 2021: p. accepted for publication.
14. Pielichowska, K. and K. Pielichowski, *Phase change materials for thermal energy storage.* Progress in Materials Science, 2014. **65**: p. 67-123.
15. Fredi, G., et al., *Wax Confinement with Carbon Nanotubes for Phase Changing Epoxy Blends.* Polymers 2017. **9**(9): p. 405.
16. de Gracia, A. and L.F. Cabeza, *Phase change materials and thermal energy storage for buildings.* Energy and Buildings, 2015. **103**: p. 414-419.
17. Yuan, Y., et al., *Fatty acids as phase change materials: A review.* Renewable and Sustainable Energy Reviews, 2014. **29**: p. 482-498.
18. Dorigato, A., G. Fredi, and A. Pegoretti, *Thermo-Mechanical Behavior of Novel Wood Laminae-Thermoplastic Starch Biodegradable Composites With Thermal Energy Storage/Release Capability.* Frontiers in Materials, 2019. **6**: p. 76.
19. Valentini, F., et al., *Development of eco-sustainable plasters with thermal energy storage capability.* Journal of Applied Physics, 2020. **128**(7): p. 075103.
20. Farid, M.M., et al., *A review on phase change energy storage: materials and applications.* Energy conversion and management, 2004. **45**(9-10): p. 1597-1615.
21. Castellon, C., et al., *Effect of microencapsulated phase change material in sandwich panels.* Renewable Energy, 2010. **35**(10): p. 2370-2374.
22. Rigotti, D., A. Dorigato, and A. Pegoretti, *3D printable thermoplastic polyurethane blends with thermal energy storage/release capabilities.* Materials Today Communications, 2018. **15**: p. 228-235.
23. Fallahi, E., M. Barmar, and M.H. Kish, *Preparation of Phase-change Material Microcapsules with Paraffin or Camel Fat Cores: Application to Fabrics.* Iranian Polymer Journal, 2010. **19**(4): p. 277-286.
24. Salaün, F., et al., *Preparation and characteristics of n-nonadecane/cement composites as thermal energy storage materials in buildings.* Thermochimica acta, 2010. **506**: p. 82-93.
25. Fredi, G., A. Dorigato, and A. Pegoretti, *Multifunctional glass fiber/polyamide composites with thermal energy storage/release capability.* eXPRESS Polymer Letters, 2018. **12**(4): p. 349-364.
26. He, B., V. Martin, and F. Setterwall, *Phase transition temperature ranges and storage density of paraffin wax phase change materials.* Energy, 2004. **29**(11): p. 1785-1804.
27. Sharma, A., et al., *Review on thermal energy storage with phase change materials and applications.* Renewable and Sustainable Energy Reviews, 2009. **13**(2): p. 318-345.
28. Fredi, G., et al., *Docosane-Organosilica Microcapsules for Structural Composites with Thermal Energy Storage/Release Capability.* Materials, 2019. **12**(8): p. 1286.
29. Regin, A.F., S.C. Solanki, and J.S. Saini, *Heat transfer characteristics of thermal energy storage system using PCM capsules: A review.* Renewable and Sustainable Energy Reviews, 2008. **12**(9): p. 2438-2458.
30. Phadungphatthanakoon, S., S. Poompradub, and S.P. Wanichwecharungruang, *Increasing the Thermal Storage Capacity of a Phase Change Material by Encapsulation: Preparation and Application in Natural Rubber.* Applied Materials & Interfaces, 2011. **3**(9): p. 3691-3969.

31. Dorigato, A., et al., *Phase changing nanocomposites for low temperature thermal energy storage and release.* eXPRESS Polymer Letters, 2017. **11**(9): p. 738-752.

32. Hong, Y. and G. Xin-shi, *Preparation of polyethylene–paraffin compound as a form-stable solid-liquid phase change material.* Solar energy materials and solar cells, 2000. **64**(1): p. 37-44.

33. Krupa, I., G. Mikova, and A.S. Luyt, *Polypropylene as a potential matrix for the creation of shape stabilized phase change materials.* European polymer journal, 2007. **43**(3): p. 895-907.

34. Sari, A., et al., *Poly(ethylene glycol)/poly(methyl methacrylate) blends as novel form-stable phase-change materials for thermal energy storage.* Journal of applied polymer science, 2009. **116**(2): p. 929-933.

35. Cao, Q. and L. Pengsheng, *Hyperbranched polyurethane as novel solid–solid phase change material for thermal energy storage.* European polymer journal, 2006. **42**(11): p. 2931-2939.

36. Kaygusuz, K., et al., *Encapsulated Fatty Acids in an Acrylic Resin as Shape-stabilized Phase Change Materials for Latent Heat Thermal Energy Storage.* Energy Sources, Part A: Recovery, Utilization, and Environmental Effects, 2008. **30**.

37. Mohebbi, A., et al., *Current Issues and Challenges in Polypropylene Foaming: A Review.* Cellular polymers, 2015. **34**(6).

38. Eaves, D., *Handbook of Polymer Foams*. 2004: Rapra Technology Ldt.

39. Mills, N., *Polymer Foams Handbook: Engineering and Biomechanics Applications and Design Guide*. 2007: Butterworth-Heinemann. 3 - 5.

40. Rodriguez-Perez, M.A., et al., *Mechanical Characterization of Closed-Cell Polyolefin Foams.* Journal of Applied Polymer Science, 2000 **75**: p. 156-166.

41. Stehr, J., *Chemical blowing agents in the rubber industry . Past – present – and future ?* Gummi Fasern Kunststoffe, 2015. **68**(12): p. 821-819.

42. Michaeli, W. and S. Sitz, *Analysis of the Expansion Behaviour of Rubber Compounds with Chemical Blowing Agents.* Cellular Polymers, 2010. **29**(4): p. 227-236.

43. Hopmann, C., F. Lemke, and Q. Nguyen Binh, *Foaming of EPDM with water as blowing agent in injection molding.* Journal of Applied Polymer Science, 2016. **133**(27): p. 1-11.

44. Han, C.D. and C.A. Villamizar, *Studies on structural foam processing I. The rheology of foam extrusion.* Polymer Engineering & Science, 1978. **18** (9): p. 687-698.

45. Kropp , D., et al., *Foam Extrusion of Thermoplastic Elastomers Using CO_2 as Blowing Agent.* Journal of cellular plastics, 1998: p. 304-311.

46. Gendron, R., et al., *Foaming Polystyrene with a Mixture of CO2 and Ethanol.* Journal of cellular plastics, 2006: p. 127-138.

47. Oh, S.H., et al., *Fabrication and characterization of hydrophilic poly(lactic-coglycolic acid)/poly(vinyl alcohol) blend cell scaffolds by*

melt-molding particulate-leaching method. Biomaterials, 2003. **24**: p. 4011-4021.

48. Scaffaro, R., et al., *Melt Processed PCL/PEG Scaffold With Discrete Pore Size Gradient for Selective Cellular Infiltration.* Macromolecular Materials and Engineering, 2016. **301**(2): p. 182-190.

49. Scaffaro, R., et al., *Preparation of three-layered porous PLA/PEG scaffold: relationship between morphology, mechanical behavior and cell permeability.* Journal of the Mechanical Behavior of Biomedical Materials, 2016. **54**: p. 8-20.

50. Mosanenzadeh, S.G., et al., *Development, characterization, and modeling of environmentally friendly open-cell acoustic foams.* Polymer Engineering & Science, 2013. **53**(9): p. 1979-1989.

51. Scaffaro, R., et al., *Integration of PCL and PLA in a monolithic porous scaffold for interface tissue engineering Author links open overlay panel.* Journal of the Mechanical Behavior of Biomedical Materials, 2016. **63**: p. 303-313.

52. Kroon, R., et al., *Bulk Doping of Millimeter-Thick Conjugated Polymer Foams for Plastic Thermoelectrics.* Advanced Functional Materials, 2017. **27**(47): p. 1704183.

53. Trakanpruk, W. and Y. Rodthong, *Production of Sponge Rubber for Monolayer Rubber Stamp Using Salt Leaching Method.* Journal of Metals, Materials and Minerals, 2008. **18**(2): p. 33-40.

54. Zonta, E., et al., *Evaluation of the salt leaching method for the production of EPDM rubber foams.* Polymer Engineering & Science, 2021. **61**(1): p. 136-153.

55. Valentini, F., et al., *Production and Characterization of TES-EPDM Foams With Paraffin for Thermal Management Applications.* Frontiers in Materials, 2021. **8**: p. 101.

56. Chen, Q., et al., *3D Printed Multifunctional, Hyperelastic Silicone Rubber Foam.* Advanced Functional Materials, 2019. **29**(23): p. 1900469.

57. Hou, Q., D.W. Grijpma, and J. Feijen, *Porous polymeric structures for tissue engineering prepared by a coagulation, compression moulding and salt leaching technique.* Biomaterials, 2003. **24**(11): p. 1937-1947.

58. Scaffaro, R., et al., *Mechanical behavior of polylactic acid/polycaprolactone porous layered functional composites.* Composites Part B: Engineering, 2016. **98**: p. 70-77.

59. Chilali, A., et al., *Effect of geometric dimensions and fibre orientation on 3D moisture diffusion in flax fibre reinforced thermoplastic and thermosetting composites.* Composites Part A: Applied Science and Manufacturing, 2017. **95**: p. 75-86.

60. Alvarez, F.X., D. Jou, and A. Sellitto, *Pore-size dependence of the thermal conductivity of porous silicon: A phonon hydrodynamic approach.* Applied physics letters, 2010. **97**(3).

61. Fredi, G., A. Dorigato, and A. Pegoretti, *Novel reactive thermoplastic resin as a matrix for laminates containing phase change microcapsules.* Polymer composites, 2019. **40**(9): p. 3711-3724.

62. Fredi, G., et al., *Detailed experimental and theoretical investigation of the thermomechanical properties of epoxy composites containing paraffin microcapsules for thermal management.* Polymer Engineering & Science, 2020. **60**(6): p. 1202-1220.

List of Figures

List of Tables

Figures

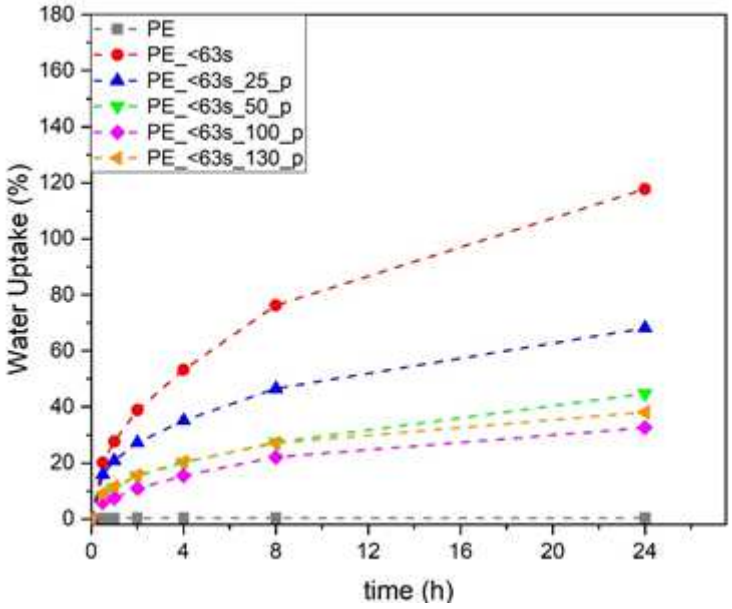

Figure 1

Results of the water uptake measurements on the prepared foams.

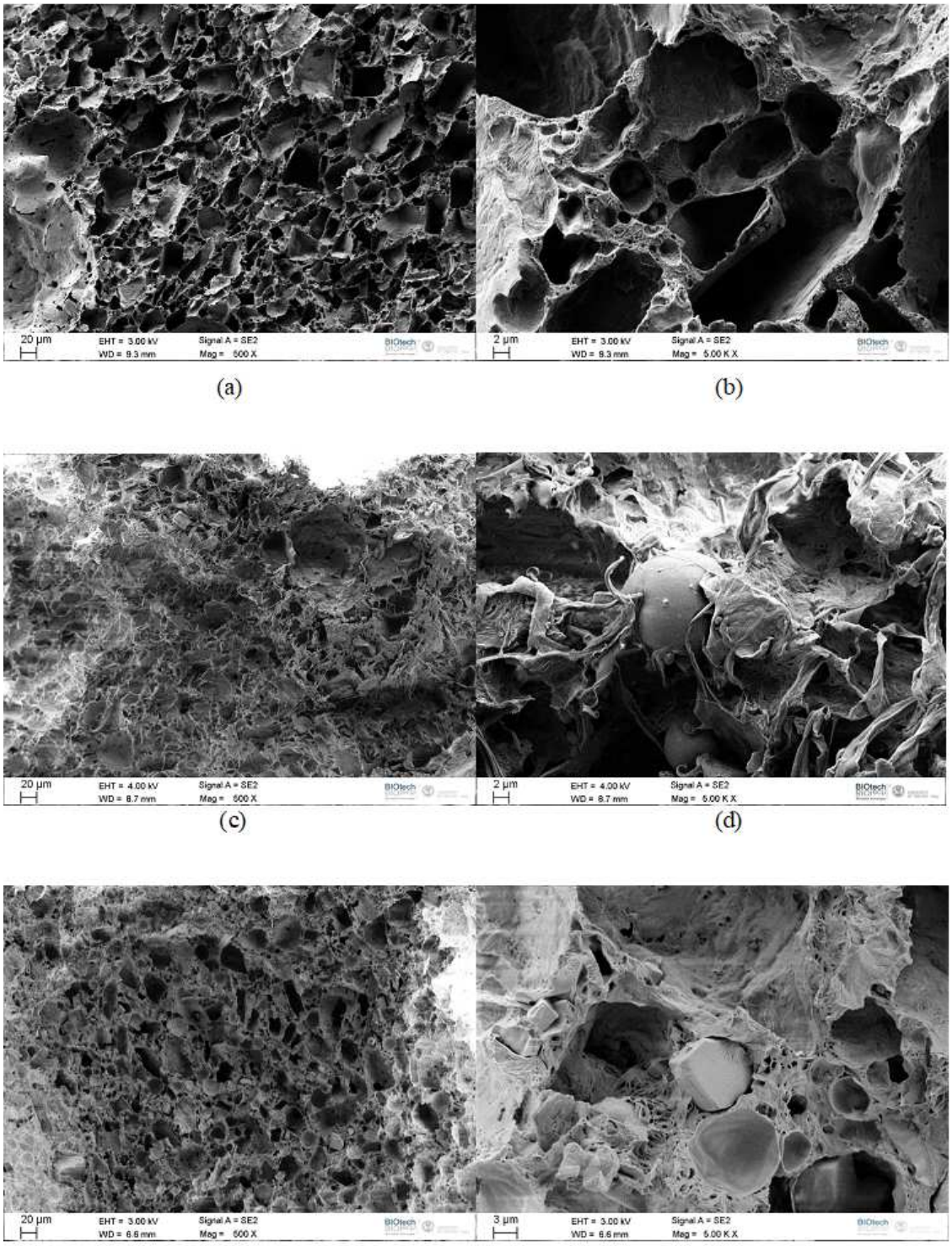

Figure 2

SEM micrographs of the prepared foams: (a) PE_<63s, 500x; (b) PE_<63s, 5000 x; (c) PE_<63s_50p, 500x; (d) PE_<63s_50p, 5000x, (e) PE_<63s_130p, 500x; (f) PE_<63s_130p, 5000x

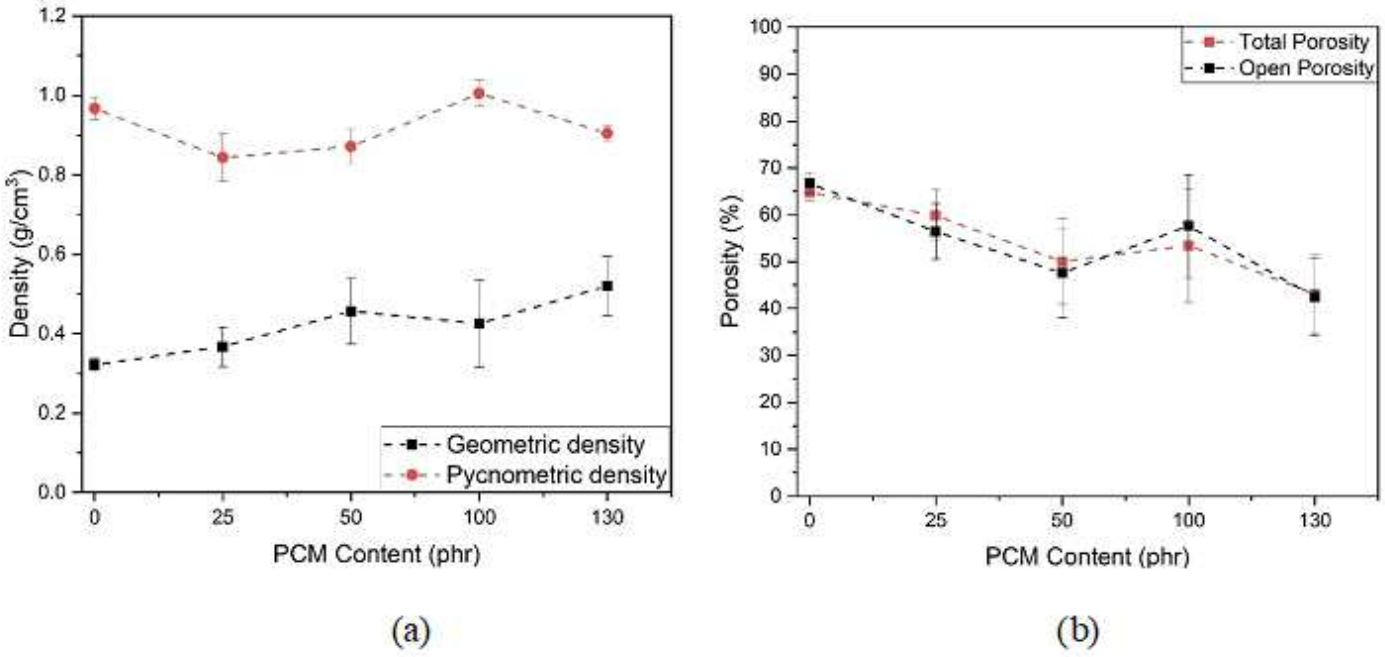

Figure 3

Results of density measurements: (a) geometric and pycnometric density, (b) porosity content.

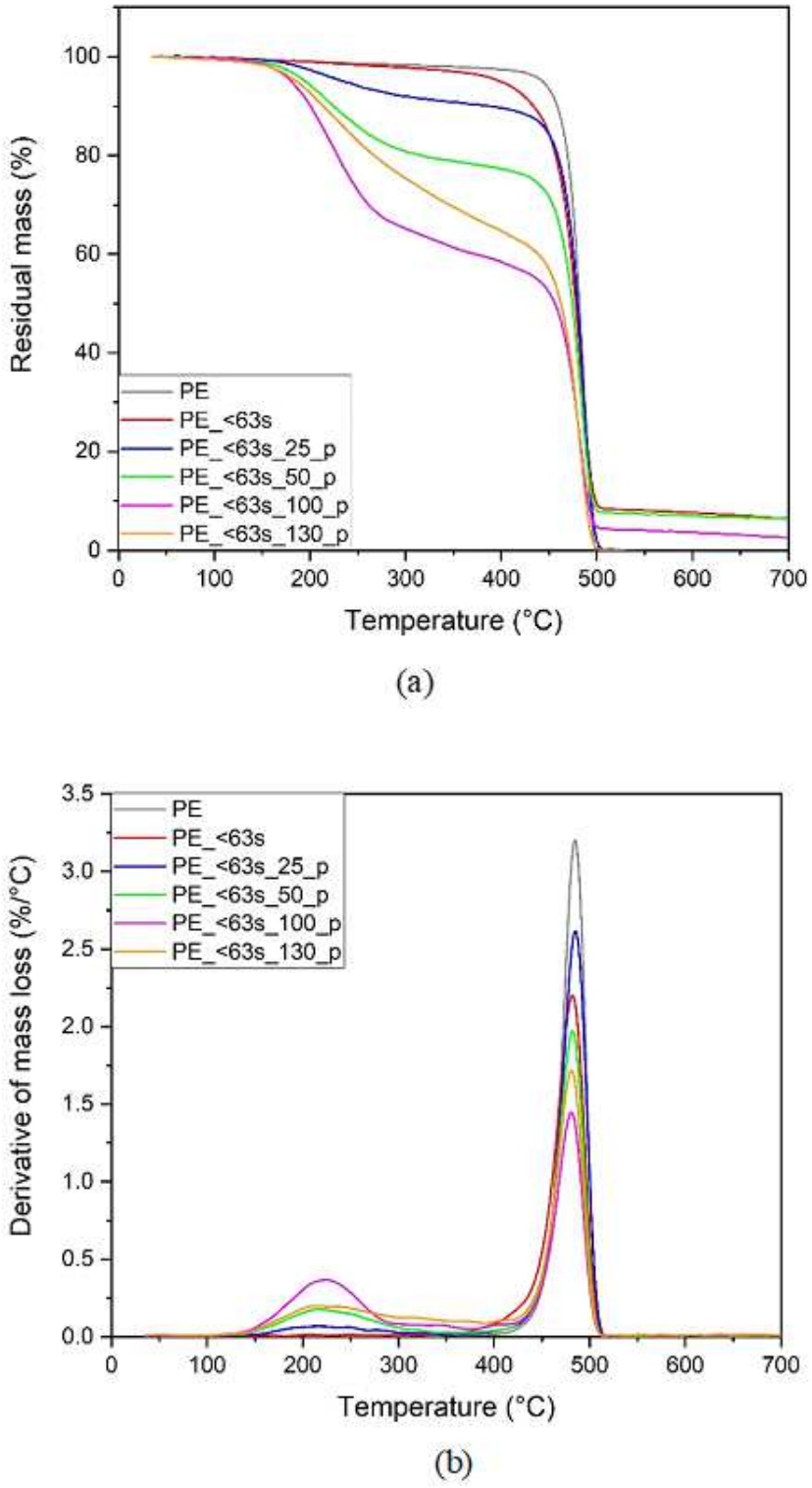

Figure 4

Residual mass (a) and derivative of mass loss (b) from TGA tests on the prepared samples.

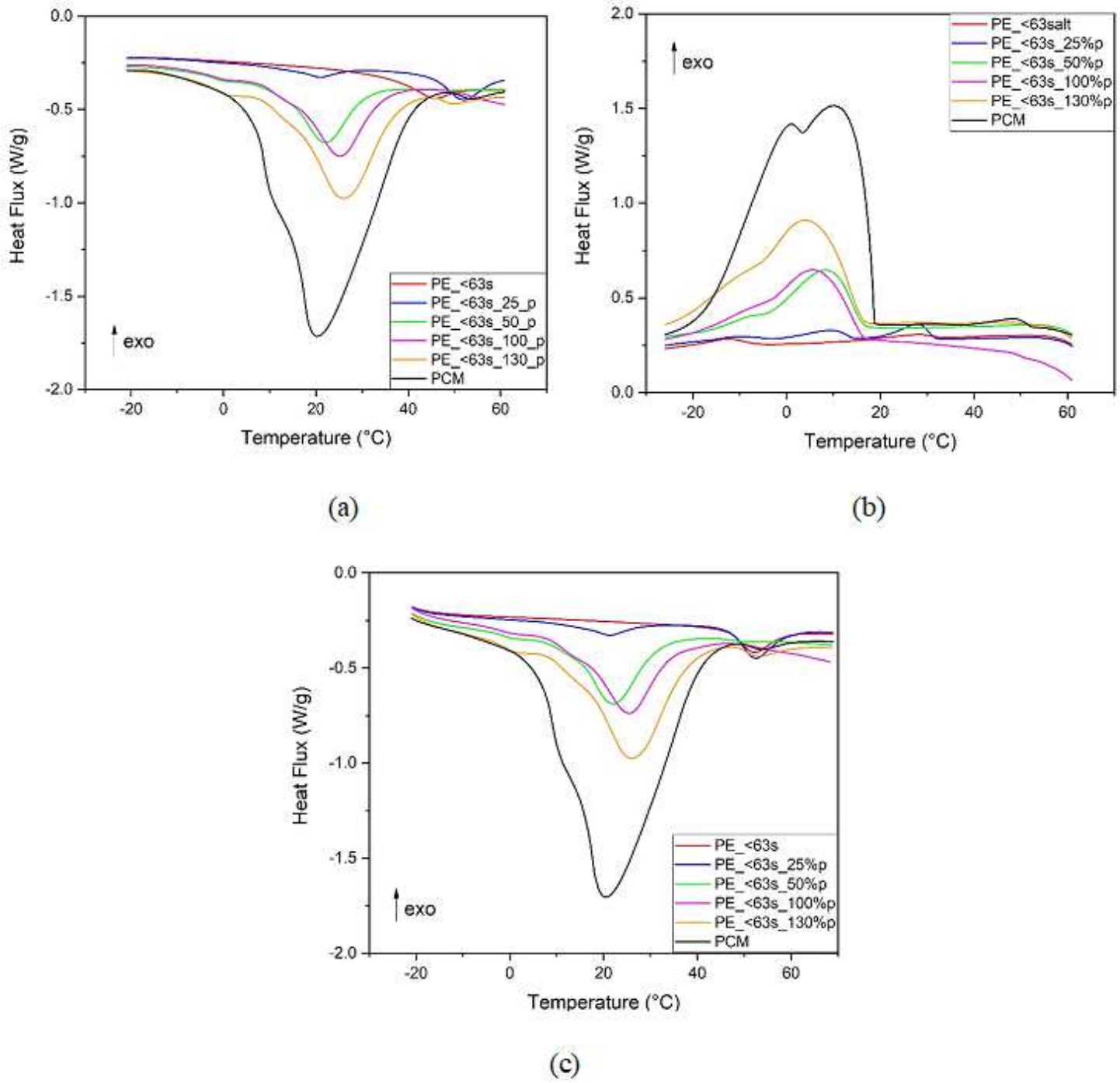

Figure 5

DSC thermograms of the prepared foams and of the neat PCM: (a) first heating, (b) cooling and(c) second heating scan.

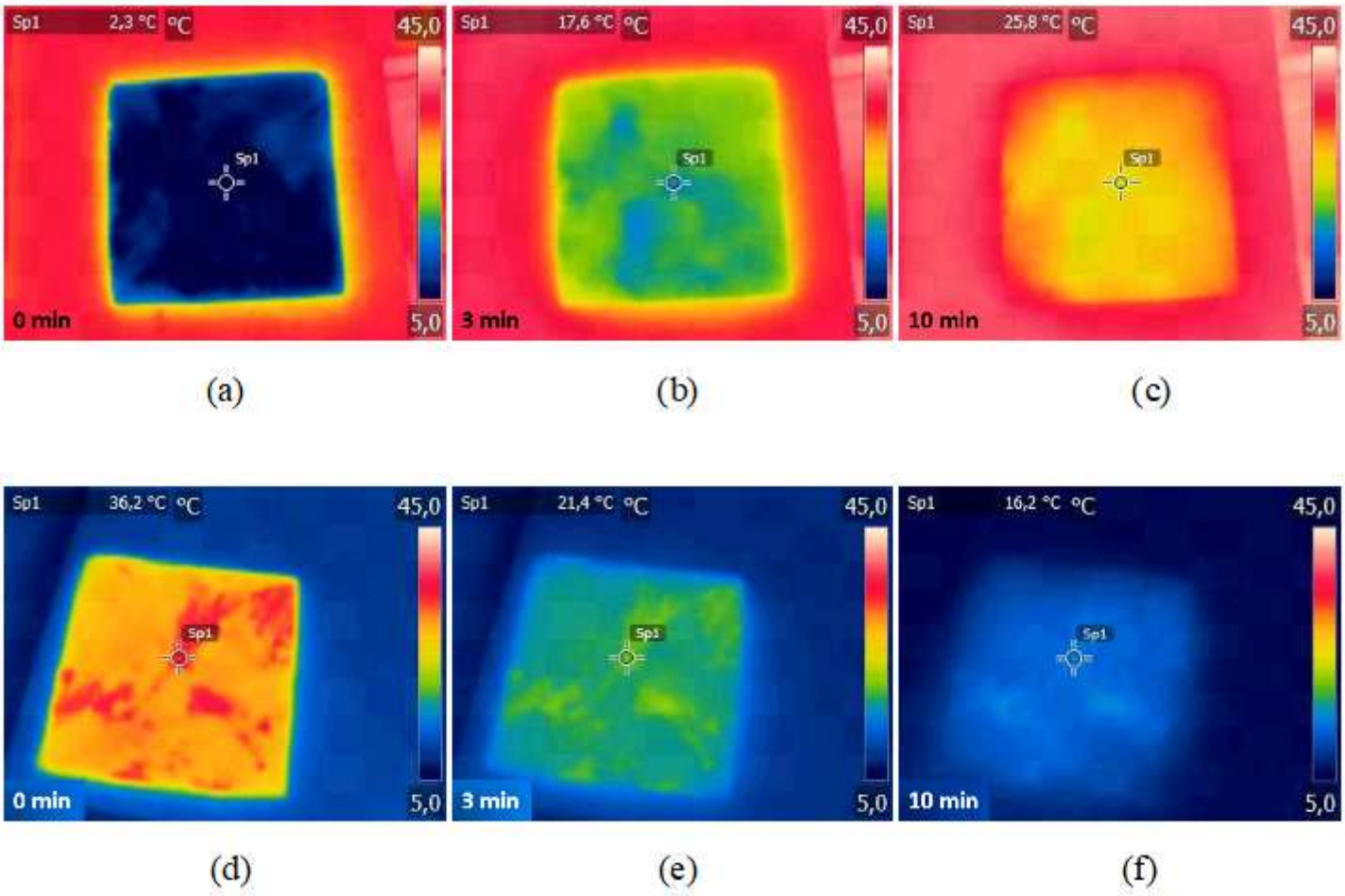

Figure 6

IR thermography images after 0, 3 and 10 minutes of PE_<63s_130_pfoam during heating (a-c) and cooling (d-e) stages.

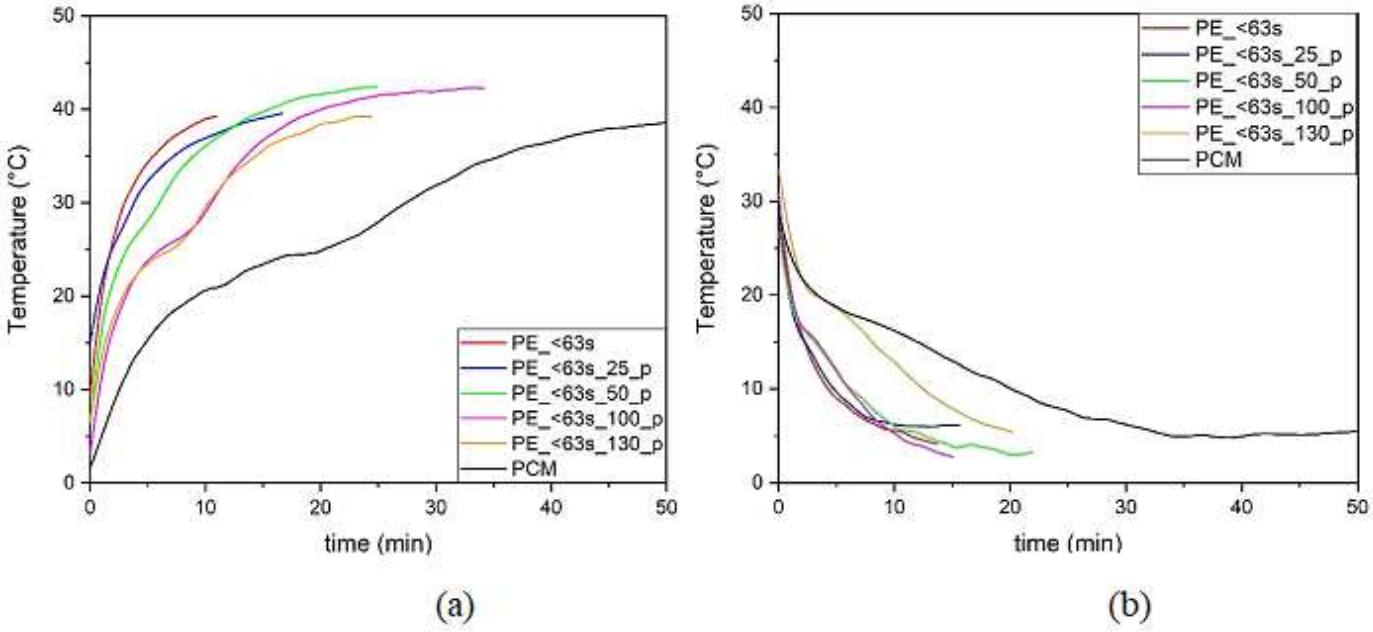

Figure 7

Temperature profiles obtained from thermal imaging tests on the prepared foams during (a) heating and (b) cooling stages.

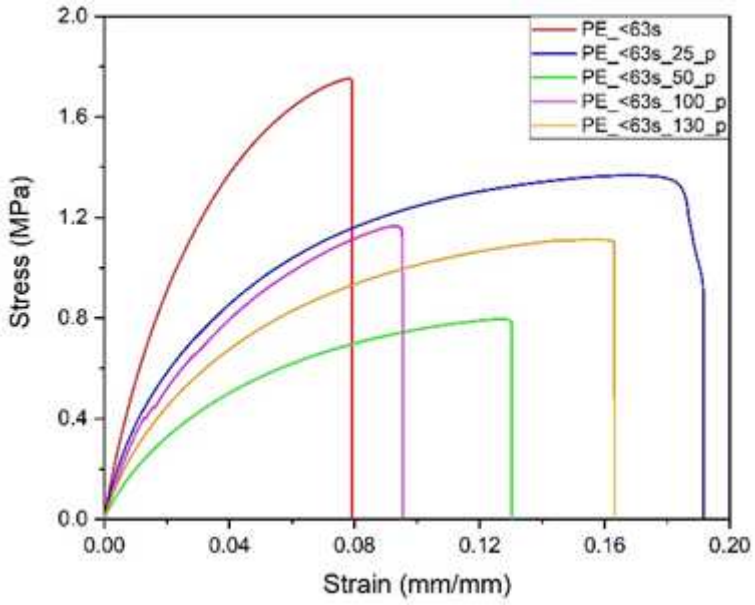

Figure 8

Representative stress-strain curves from quasi-static tensile tests on the prepared foams.